Epigenome programing by H3.3K27M mutation creates a dependence of pediatric glioma on SMARCA4

Yan Mo[1,2,3,4,8], Shoufu Duan[1,2,3,4,8], Xu Zhang[1,2,3,4,8], Xu Hua[1,2,3,4], Hui Zhou[1,2,3,4], Hong-Jian Wei[5], Jun Watanabe[6], Nicholas McQuillan[5], Zhenyi Su[1,2,7], Wei Gu[1,2,7], Cheng-Chia Wu[5], Christopher R. Vakoc[8], Rintaro Hashizume[6], Kenneth Chang[8], and Zhiguo Zhang[1,2,3,4,*]

[1]Institute for Cancer Genetics, Columbia University Irving Medical Center, New York, NY 10032, USA

[2]Herbert Irving Comprehensive Cancer Center, Columbia University Irving Medical Center, New York, NY 10032, USA

[3]Department of Pediatrics, Columbia University Medical Center, New York, NY 10032, USA

[4]Department of Genetics and Development, Columbia University Medical Center, New York, NY 10032, USA.

[5]Department of Radiation Oncology, Columbia University Irving Medical Center, New York, NY 10032, USA

[6]Department of Pediatrics, Northwestern University Feinberg School of Medicine, Chicago, IL 60611, USA.

[7]Department of Pathology and Cell Biology, Columbia University Irving Medical Center, New York, NY 10032, USA

[8]Cold Spring Harbor Laboratory, Cold Spring Harbor, NY 11724, USA

[8]These authors contribute equally to this work.

*Corresponding author and lead contact: Zhiguo Zhang, 1130 St. Nicolas Ave, ICRC 407A, New York, New York 10032. Phone number: 212-851-4936

E-mail: zz2401@cumc.columbia.edu

Running title: DIPG tumors depend on SMARCA4

Declaration of Interests: The authors declare no competing interests.

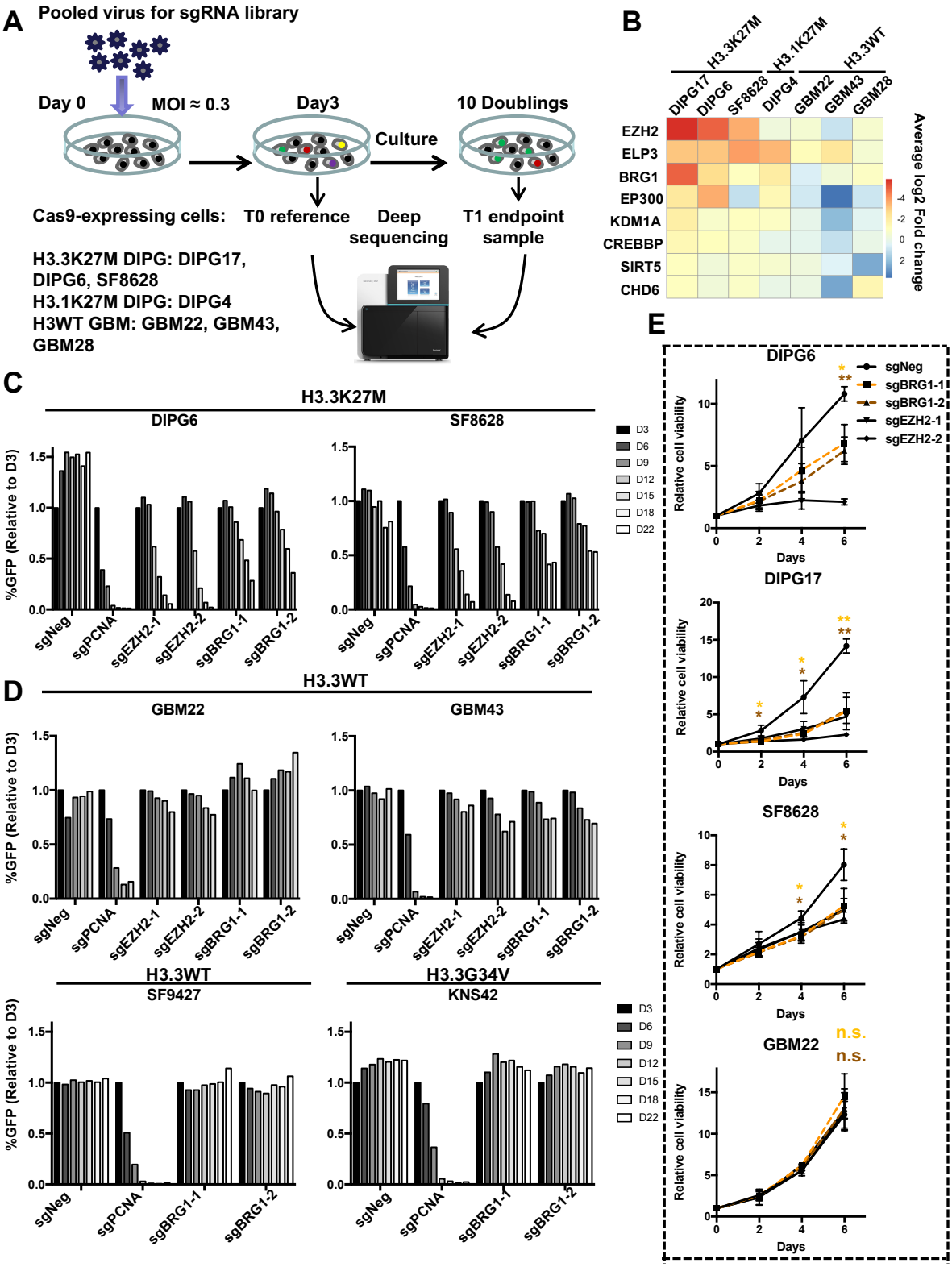
A
Pooled virus for sgRNA library
Day 0
MOI ≈ 0.3
Day3
Culture
10 Doublings
Cas9-expressing cells:
T0 reference
Deep sequencing
T1 endpoint sample
H3.3K27M DIPG: DIPG17, DIPG6, SF8628
H3.1K27M DIPG: DIPG4
H3WT GBM: GBM22, GBM43, GBM28
B
H3.3K27M
H3.1K27M
H3.3WT
DIPG17
DIPG6
SF8628
DIPG4
GBM22
GBM43
GBM28
EZH2
ELP3
BRG1
EP300
KDM1A
CREBBP
SIRT5
CHD6
Average log2 Fold change
C
H3.3K27M
DIPG6
SF8628
%GFP (Relative to D3)
sgNeg
sgPCNA
sgEZH2-1
sgEZH2-2
sgBRG1-1
sgBRG1-2
D
H3.3WT
GBM22
GBM43
H3.3WT
SF9427
H3.3G34V
KNS42
D3
D6
D9
D12
D15
D18
D22
E
DIPG6
DIPG17
SF8628
GBM22
Relative cell viability
Days
sgNeg
sgBRG1-1
sgBRG1-2
sgEZH2-1
sgEZH2-2
n.s.
n.s.

Supplementary Fig. S1. DMG cells are vulnerable to SMARCA4 depletion.
(A) An outline of the CRISPR/Cas9 screen. H3K27M DMG cell lines (DIPG6, DIPG17, SF8628 and DIPG4) and H3 WT cells (GBM22, GBM43 and GBM28) expressing Cas9 were transduced with the "epigenetic" library at MOI~0.3 and were collected at day 3 after infection (T0) and after 10 doubling of each line (T1). The sgRNA abundance at T1 and T0 in each cell line was analyzed by next generation sequencing.

(B) Heatmap of sgRNA abundance, represented by $\log_2$ fold change (T1/T0), of candidate genes identified in the screen.

(C-D) Effects of SMARCA4 depletion on the proliferation of DMG cells using a competition assay. The experiments were performed as described in Fig. 1A.

(E) Effects of SMARCA4 depletion on the proliferation of H3K27M (DIPG6, DIPG17, SF8628) and H3 WT (GBM22) cells based on cell viability assays. EZH2 KO (sgEZH2-1 and sgEZH2-2) was used as a positive control in DMG cells. The results were the average and SD from three independent repeats (two-tailed Students' test, n.s., not significant, * $p<0.05$, ** $p<0.01$).

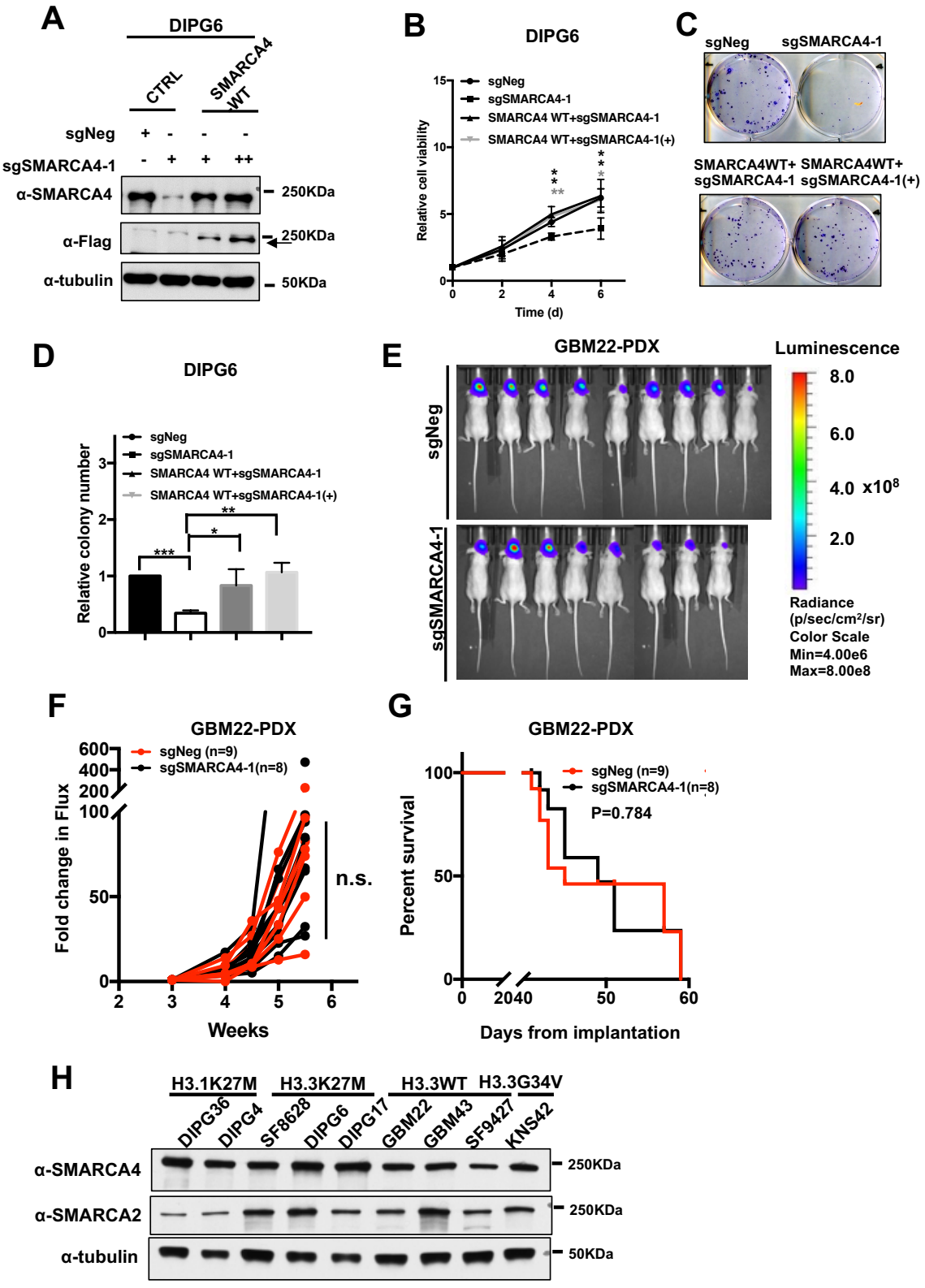

Supplementary Fig. S2. Exogenous expression of SMARCA4 rescues the proliferation defects of DIPG6 cells induced by SMARCA4 depletion.

(A-D) Exogenous expression of SMARCA4 in DIPG6 cells from the sgSMARCA4-1 resistant construct rescues the proliferation defects upon depletion of endogenous SMARCA4. The experiments were performed as described in Fig. 2 except that DIPG6 cells were used. +: two rounds of viral infection with sgSMARCA4-1.

(E-F) Depletion of SMARCA4 does not affect the growth of GBM22 xenografts *in vivo*. GBM22 cells expressing firefly luciferase were infected with lentivirus expressing sgSMARCA4-1 or sgNeg and were implanted in the supratentorial brain of female mice. After 3 weeks of implantation, tumor growth of GBM22 xenografts were monitored by bioluminescent imaging (BLI), with representative BLI at week 4.5 shown in (E) and bioluminescent signals at different time points normalized against week 3 shown in (F). (n.s., not significant, two-tailed Students' test).

(G) Survival curves of mice xenografted with GBM22 cells with sgNeg or with sgSMARCA4-1 (sgNeg: n= 9 mice, sgSMARCA4-1: n= 8 mice).

(H) Western blot analysis of protein levels of SMARCA4 and SMARCA2 in five DMG cell lines and four GBM cell lines without H3K27M mutation.

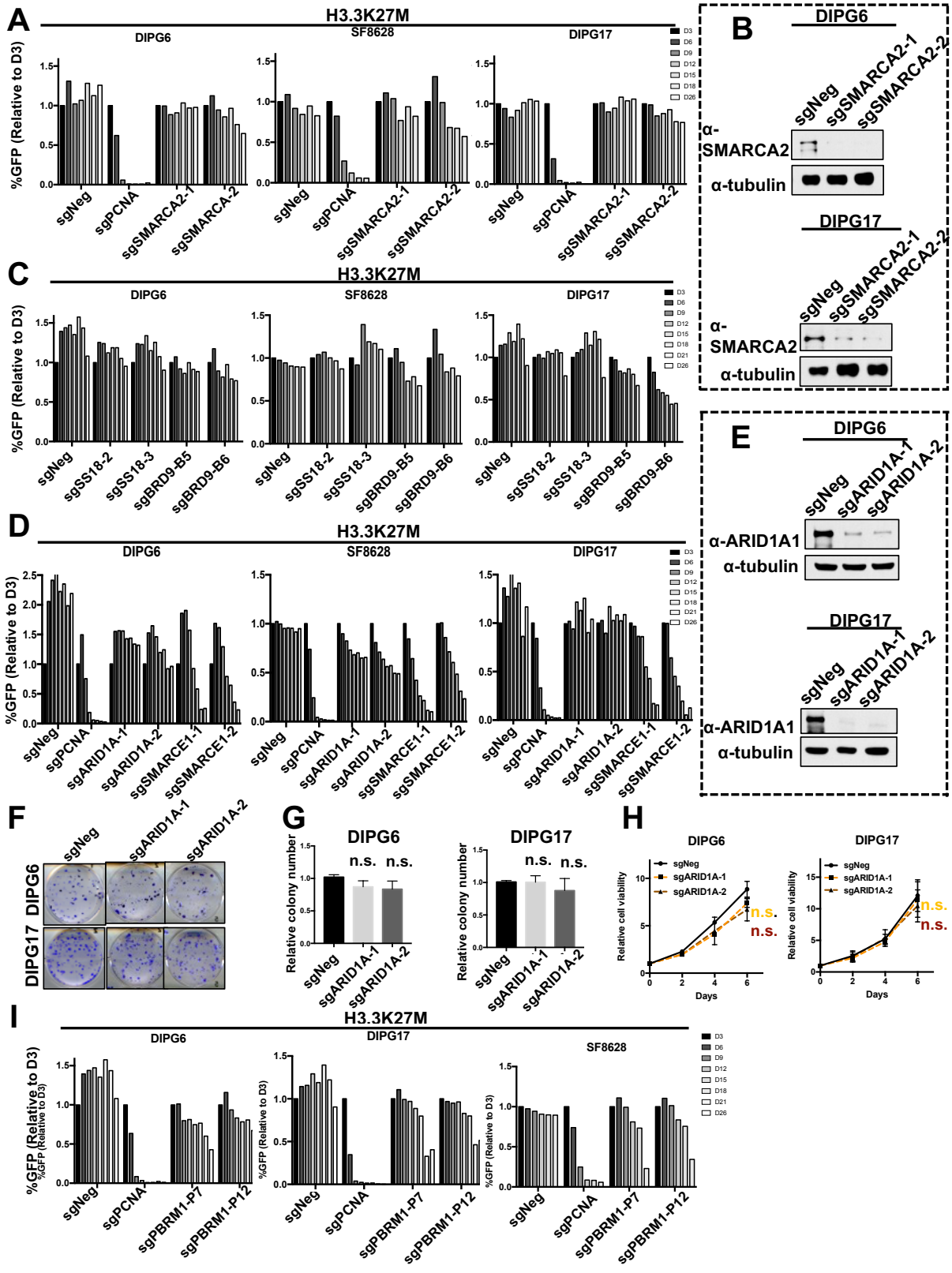

Supplementary Fig. S3. Effects of depletion of SMARCA2 and five subunits of the mammalian SWI/SNF complex on the proliferation of DMG cells.

(A-B) Effect of SMARCA2 depletion on the proliferation of DMG cells. (A) GFP depletion assays in DMG cells were performed using two sgRNAs targeting SMARCA2 (sgSMARCA2-1 and sgSMARCA2-2). (B) SMARCA2 proteins were depleted in DIPG6 and DIPG17 cells by two sgRNAs and were analyzed by Western blot.

(C-D) Effects of depletion of SS18 and BRD9 (C), ARID1A and SMARCE1 (D), on the proliferation of DMG cells. The experiments in A C and D were performed essentially the same as described in Fig. 1A.

(E-H) Effects of ARID1A depletion on the proliferation of H3K27M DMG cells. DIPG6 and DIPG17 cells were infected with lentivirus expressing two sgRNA targeting ARID1A (sgARID1A-1 and sgARID1A-2) and negative control (sgNeg). Cells were collected for Western blot analysis using antibodies against ARID1A with Tubulin as controls (E), and for colony formation assays with representative images shown in (F) and the results from three independent repeats shown in (G), and for cell viability assays (H). The results were the average and SD from three independent repeats (n.s., not significant, $p>0.05$, two-tailed Students' test).

(I) Effects of depletion of PBRM1 on three DMG cell lines based on GFP-based competition assays. The experiments were performed essentially the same as described in Fig. 1A.

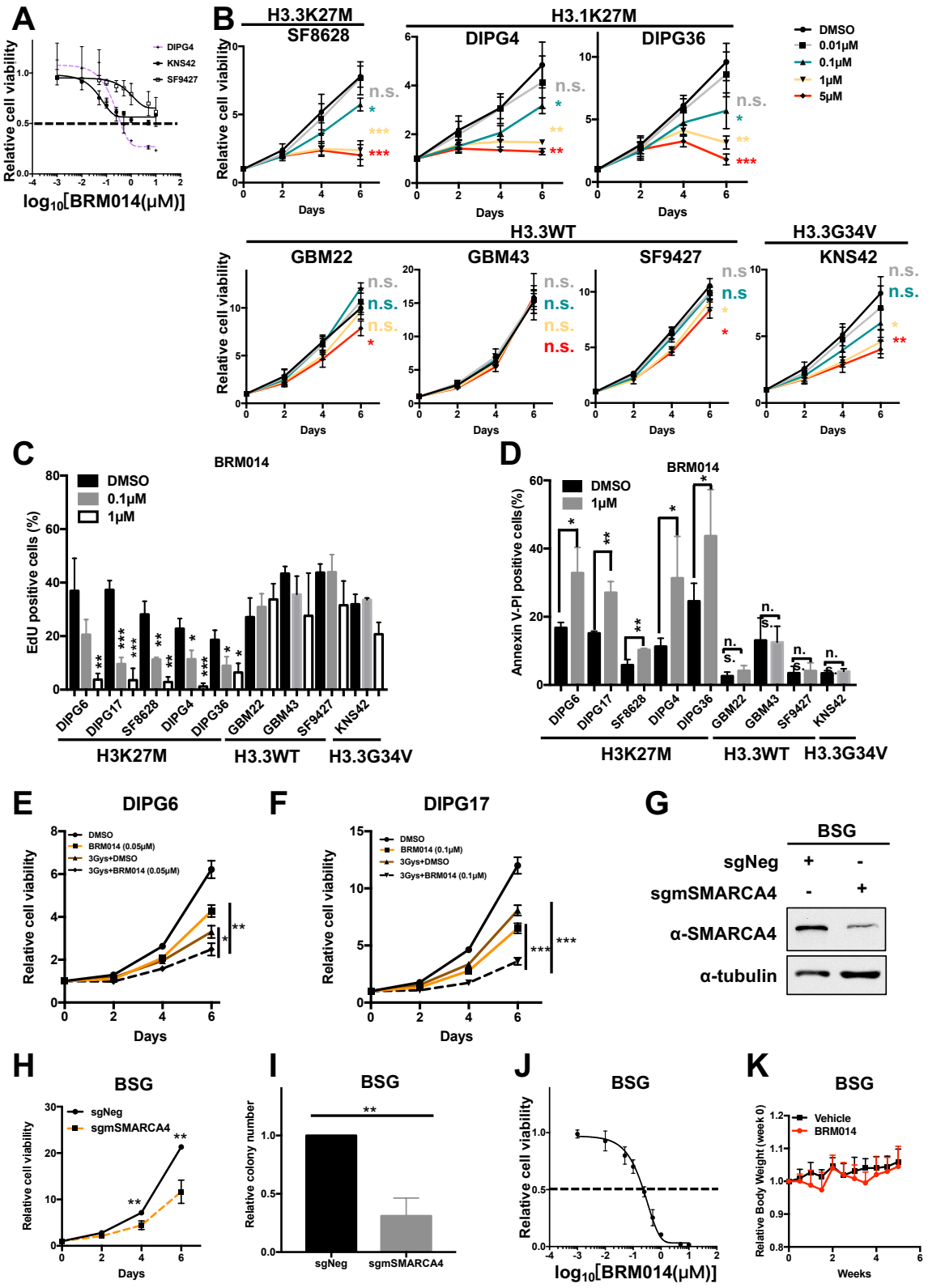

Supplemental Figure 4. Effects of BRM014 treatments on both human and mouse DMG cell lines.

(A-B) Effects of BRM014 treatment on the cell proliferation of indicated DMG cell lines and GBM cell lines. The results were the average and SD from three independent repeats (* $p<0.05$, ** $p<0.01$, *** $p<0.001$).

(C-D) Effect of BRM014 treatment on DNA synthesis and apoptosis of five DMG cell lines and four glioma lines. DMG cells (DIPG6, DIPG17, SF8628, DIPG4 and DIPG36) and H3 WT GBM (GBM22, GBM43, SF9427) and H3.3 G34V (KNS42) cells were treated with BRM014 at indicated dose for 6 days and used for analysis of DNA synthesis by Ethynnyl-2'-dexyuridine (EdU) incorporation (C) and for monitoring apoptosis by Annexin V/PI staining analysis (D). Results from three independent repeats were shown (* $p<0.05$, ** $p<0.01$, *** $p<0.001$, two-tailed Students' test).

(E-F) Effects of combined treatments of BRM014 and radiation on the proliferation of two DMG lines (DIPG6 (E), and DIPG17 (F)). DIPG6 and DIPG17 cells were seeded in 96 well plate and treated with radiation alone or in combination with BRM014 with indicated doses. The results were the average and SD from three independent repeats ((* $p<0.05$, ** $p<0.01$, *** $p<0.001$).

(G-I) Effects of SMARCA4 depletion on H3.3K27M murine brain stem glioma (BSG) cells (a murine model of H3.3K27M DMG). After infection with lentivirus targeting mouse SMARCA4 (sgmSMARCA4) and negative control (sgNeg), cells were collected for Western blot analysis (G), cell viability assay (H) and colony formation assay (I). The results were the average and SD from three independent repeat (** $p<0.01$).

(J) Effects of BRM014 treatment on murine BSG cell proliferation based on cell viability assays. The results were the average and SD from three independent repeats (* $p<0.05$, ** $p<0.01$, *** $p<0.001$).

(K) Effects of BRM014 treatments on body weight of athymic nude mice used in the study of Fig. 4H-I. Mean and SD of 9 mice per group were plotted.

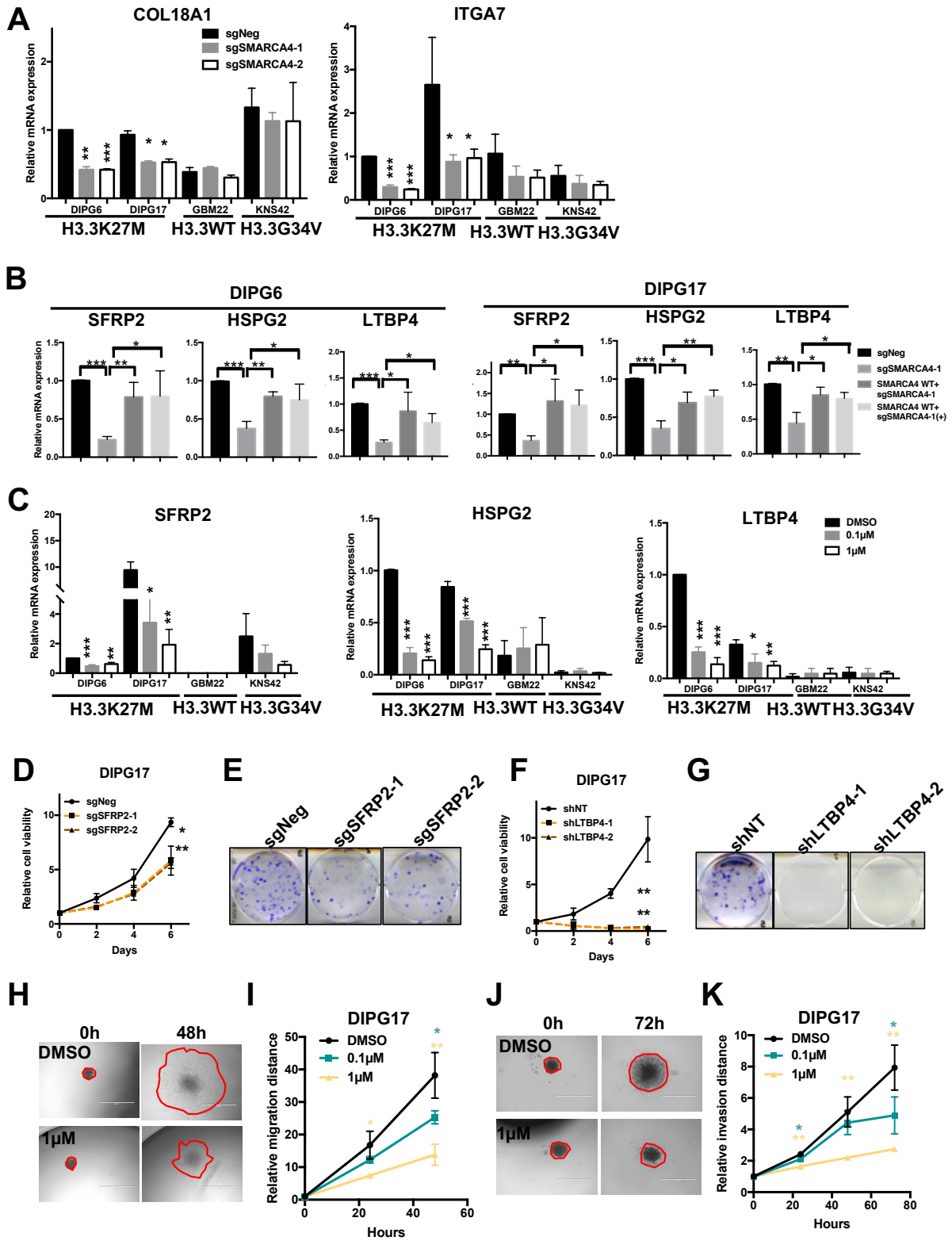

Supplementary Fig. S5. SMARCA4 regulates the expression of genes involved in extracellular matrix and cell growth.

(A) Effects of SMARCA4 depletion on the expression of two genes (COL18A1 and ITGA7) in extracellular matrix pathway in two DMG lines (DIPG6 and DIPG17) and two glioma lines (GBM22 and KNS42). RT-qPCR results from three independent experiments were shown (two-tailed Students' test, * $p<0.05$, ** $p<0.01$, *** $p<0.001$).

(B) Exogenous expression of SMARCA4 in DIPG6 (left) and DIPG17 (right) restored the reduced expression of three candidate genes tested (SFRP2, HSPG2, and LTBP4) caused by depletion of endogenous SMARCA4 in these lines. Results were from three independent experiments (* $p<0.05$, ** $p<0.01$, *** $p<0.001$). SMARCA4WT+sgSMARCA4-1(+): Cells were infected twice with lentivirus for sgSMARCA4-1.

(C) Effects of BRM014 treatment on the expression of three genes (SFRP2, HSPG2 and LTBP4) in two DMG lines (DIPG6 and DIPG17), and two glioma lines without H3K27M mutation (GBM22 and KNS42). Results were from three independent experiments (* $p<0.05$, ** $p<0.01$, *** $p<0.001$).

(D-E) Effects of SFRP2 depletion on the viability of DIPG17 cells. Cells in Fig. 4F-G were used for cell viability assays (D) and colony formation assays with represented images of colony formation assay shown in (E).

(F-G) Effects of LTBP4 depletion on the viability of DIPG17 cells. Cells in Fig. 4H-I were applied for cell viability assay (F). Represented images of colony formation assays were shown in (G).

(H-I) Effects of BRM014 treatments on the spheroid migration of DMG cells. (H) Representative images at 0 hr and 48 hr of spheroid migration assays. (I) The relative migration distance normalized against 0 hr of each sphere. The average and SD from three independent experiments were shown (* $p<0.05$, ** $p<0.01$, two-tailed Students' test).

(J-K) Effects of BRM014 treatment on the invasion of DIPG17 cells. (J) Representative images at 0 hr and 72 hr of spheroid invasion assays. (K) The relative invasion distance

normalized against 0 hr (n=3 independent experiments, **p<0.01, ***p<0.001, two-tailed Students' test).

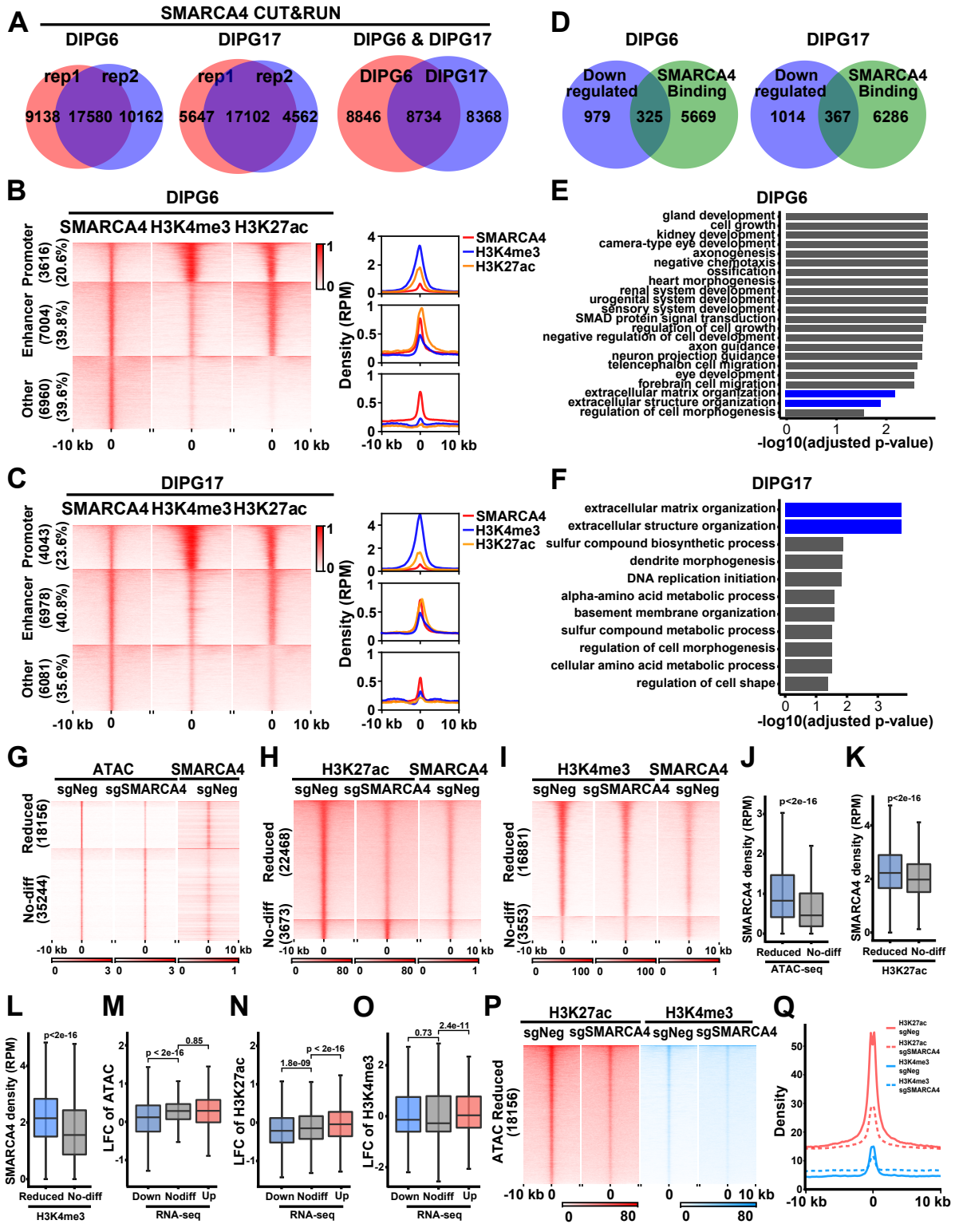

Supplementary Fig. S6. SMARCA4 co-localizes with SOX10 in DMG cells.

(A) Venn diagram showing of SMARCA4 CUT&RUN peaks identified in DIPG6 (left), DIPG17 (middle) cells from two independent experiments, and the shared peaks between DIPG6 and DIPG17 lines shown at right.

(B-C) Most SMARCA4 peaks are located at promoters and enhancers in DIPG6 (B) and DIPG17 (C) cells. SMARCA4 density and H3K4me3 CUT&RUN density and H3K27ac ChIP-seq density at each of the 17580 and 17102 SMARCA4 CUT&RUN peaks in DIPG6 and DIPG17, respectively and represented by Heatmap (left panel). The SMARCA4 peaks were separated into three groups, promoters (high levels H3K4me3), active enhancers (H3K27ac and low levels of H3K4me3) and other sites that are not promoters and active enhancers (other), with the average density of SMARCA4, H3K4me3 and H3K27ac at each of these three groups of SMARCA4 peaks in each DMG line shown at the right panel.

(D) Venn diagram of genes that were downregulated by SMARCA4 depletion in DIPG6 (left) and DIPG17 (right), and with at least one SMARCA4 peak at their promoters and/or enhancers.

(E-F) Gene ontology analysis of 325 genes down-regulated in DIPG6 and with at least one SMARCA4 CUT&RUN peaks (E), and 367 down-regulated genes in DIPG17 with at least one SMARCA4 peaks at promoter or enhancer (F).

(G) Effects of SMARCA4 depletion on chromatin accessibility in DIPG17 cells. Heatmaps of the ATAC-seq density in DIPG17 cells treated with sgNeg or sgSMARCA4 as well as SMARCA4 CUT&RUN signals at each of the ATAC-seq peaks in DIPG17 cells prior to SMARCA4 depletion. ATAC-seq assays were performed in DIPG17 cells with or without depleting SMARCA4. ATAC peaks in DIPG17 cells were divided into two groups (reduced and no-difference) based on changes in ATAC density upon SMARCA4 depletion with a cut-off of (sgSMARCA4-1/sgNeg <0.83, FDR <0.05). The ATAC-Seq density and SMARCA4

CUT&RUN signals at each ATAC-Seq peak in each group were calculated and represented by Heatmap. The average of two biological replicates were shown.

(H) Effects of SMARCA4 depletion on H3K27ac levels on chromatin in DIPG17 cells. Heatmaps representing H3K27ac CUT&RUN peaks in DIPG17 cells treated with sgNeg and sgSMARCA4, as well as SMARCA4 CUT&RUN density at these H3K27ac CUT&RUN peaks shown in the right. Reduced and no-difference represent reduced and no changes in H3K27ac CUT&RUN density upon SMARCA4 depletion with a cut-off of ((sgSMARCA4-1/sgNeg) <0.83, FDR <0.05)). The average of two biological replicates were shown.

(I) Effects of SMARCA4 depletion on H3K4me3 changes in DIPG17 cells. Heatmaps of H3K4me3 CUT&RUN density in DIPG17 cells with sgNeg or sgSMARCA4, with the SMARCA4 CUT&RUN density at these peaks shown in the right.

(J) Boxplot of SMARCA4 CUT&RUN density in DIPG17 cells prior to SMARCA4 depletion at loci with reduced (n= 18156) and no difference (n=35244) in ATAC-seq signals upon SMARCA4 depletion defined in Fig. S6G.

(K) Boxplots of SMARCA4 CUT&RUN density in DIPG17 cells treated with sgNeg at reduced and no difference H3K27ac peaks upon SMARCA4 depletion defined in Fig. 6H.

(L) Boxplots of SMARCA4 CUT&RUN density at loci with reduced H3K4me3 and without changes in H3K4me3 upon SMARCA4 depletion defined in Fig. 6I.

(M) Boxplots of Log_2 fold changes (LFC) in chromatin accessibility (Log_2 (ATAC-seq signals sgSMARCA4/sgNeg)) at TSS of three subsets of genes identified by RNA-seq in DIPG17 cells upon SMARCA4 depletion. down, No diff, and up: down-regulated, no difference, and up-regulated genes, respectively. p values were calculated by two-tailed Students' test.

(N) Boxplot of H3K27ac changes (Log_2 (H3K27ac in sgSMARCA4/H3K27ac in sgNeg) at TSS of three subsets of genes in DIPG17 cells after SMARCA4 depletion defined in (M).

(O) Boxplot of H3K4me3 changes at TSS of three subsets of genes in DIPG17 cells upon SMARCA4 depletion defined in (M).

(P-Q) H3K27ac and H3K4me3 signals at each of the 18156 reduced ATAC-seq loci in DIPG17 cells treated with sgNeg or sgSMARCA4 shown in Heatmap (P), with the average signals of shown in (Q).

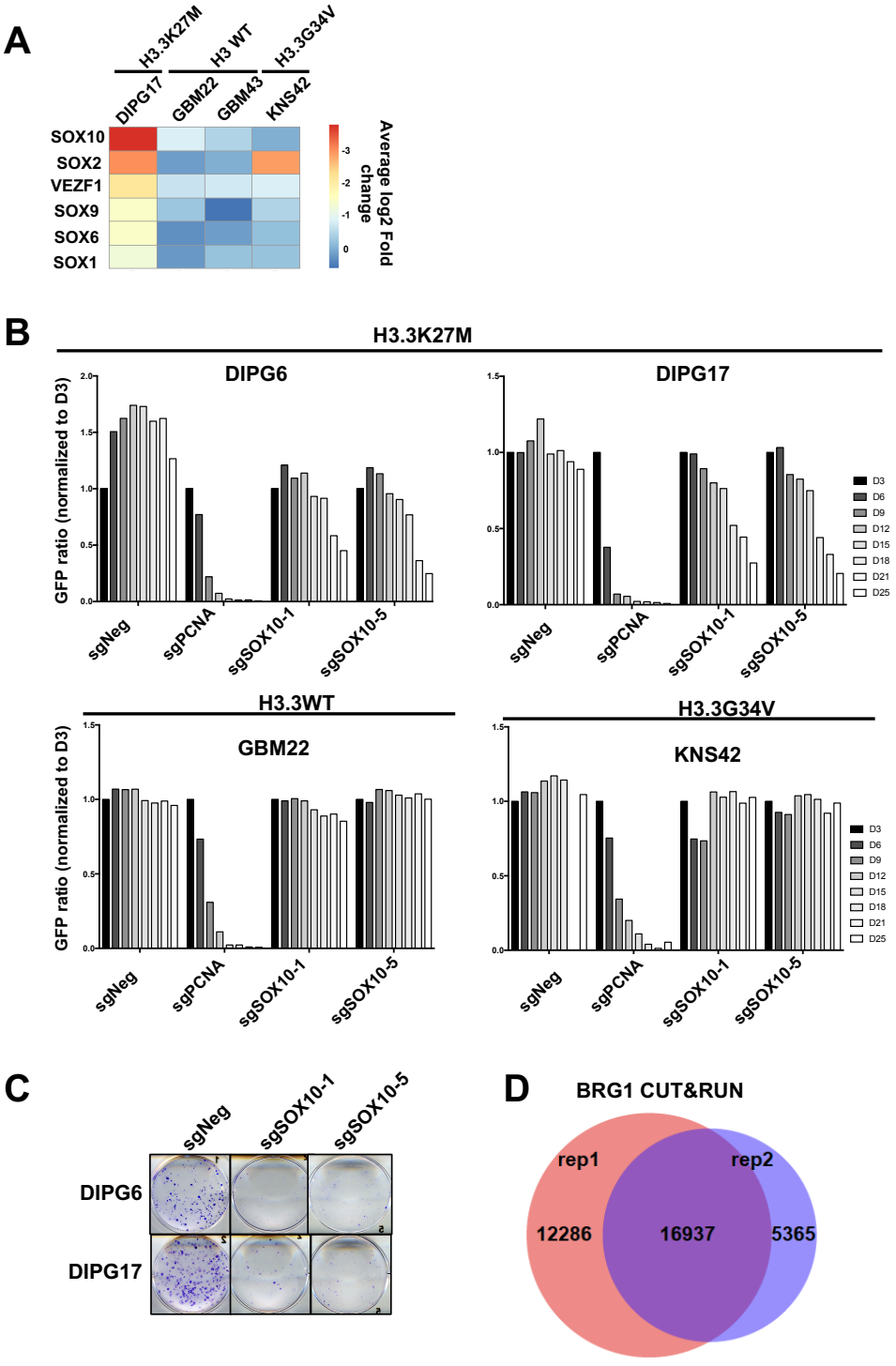

Supplementary Fig. S7. SOX10 is essential for DMG cells.

(A) SOX10 is the top candidate that inhibited the proliferation of DIPG17 cells based on an independent CRISPR/Cas9 screen using a library targeting transcription factors. Heatmaps indicate the sgRNA abundance of indicated genes based on $\log_2$ fold change (T1/T0).

(B) Effects of SOX10 depletion on the proliferation of two DMG lines (DIPG6 and DIPG17) and two glioma lines without H3K27M mutation (GBM22 and KNS42) based on the GFP-based competition assays.

(C) Representative images for colony formation assays in DIPG6 and DIPG17 cells, with quantification of the results shown in Figure 6E.

(D Venn diagram showing SMARCA4 CUT&RUN peaks identified in DIPG17 cells treated with sgNeg from two independent repeats as controls for sgSOX10 shown in Fig. 6J.

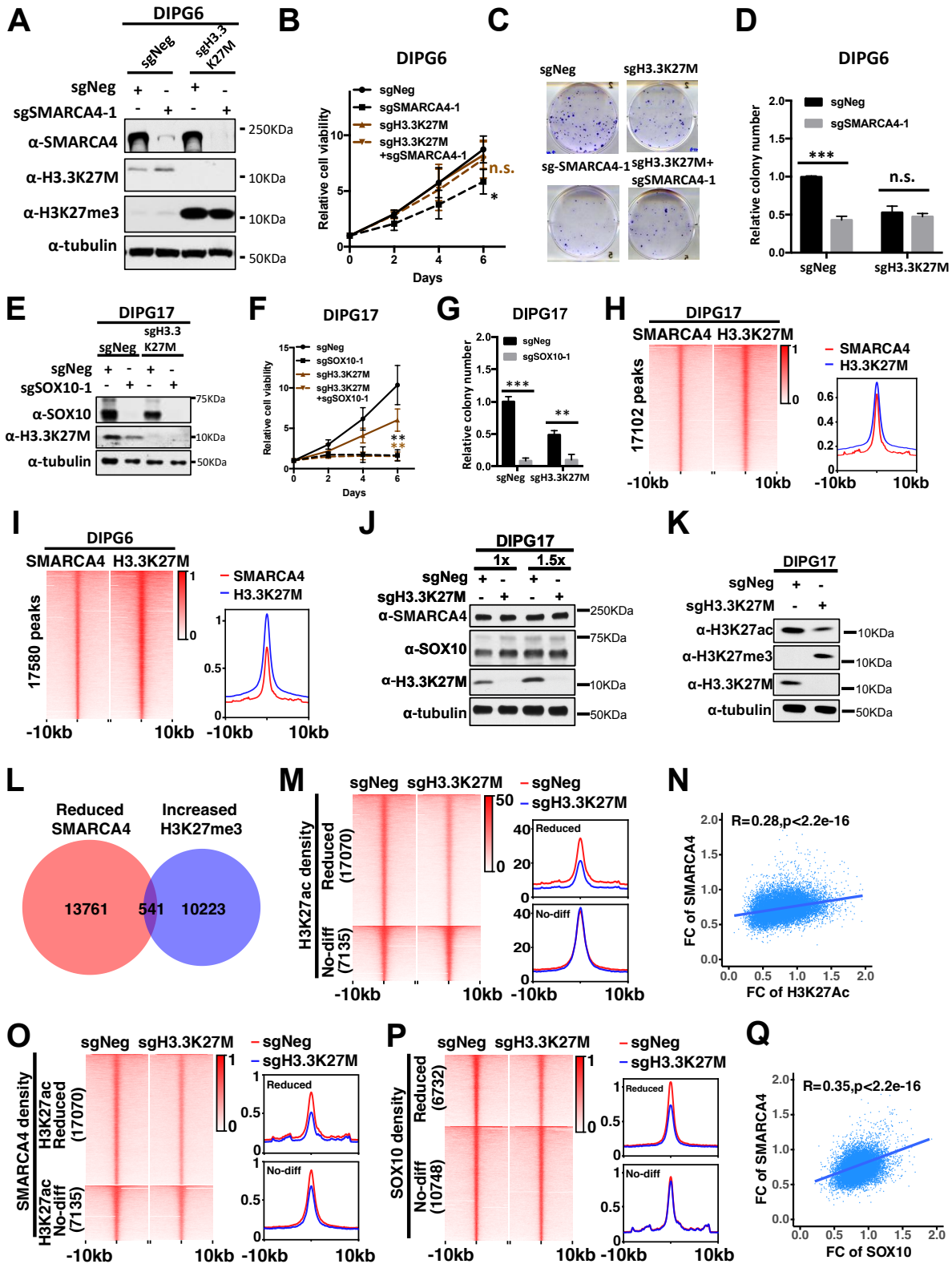

Supplementary Fig. S8. Epigenome rewiring by H3.3K27M creates a dependence of DIPG6 on SMARCA4.

(A-D) SMARCA4 depletion has no additional effects on the proliferation of H3.3K27M-depleted DIPG6 cells. The experiment was performed the same as in Fig. 7 (A-D) except that the DIPG6 cell line was used.

(E-G) Effects of SOX10 on the proliferation of DIPG17 and H3.3K27M-depleted DIPG cells. DIPG17 cells with (sgH3.3K27M) or without H3.3K27M depletion (sgNeg) were transduced with sgNeg or sgSOX10-1, and cells were collected for Western blotting analysis on indicated proteins (E), titer blue cell viability assays (F) and colony formation assays (G). The average and SD from three independent experiments were shown (*$p<0.01$, **$p<0.001$, n.s. not significant, two-tailed Students' test).

(H-I) SMARCA4 co-localizes with H3.3K27M in DMG cells. The H3.3K27M CUT&RUN density at each of 17102 SMARCA4 peaks identified in DIPG17 (H) or 17580 SMARCA4 peaks in DIPG6 (I) was calculated and represented by Heatmap, with the average SMARCA4 and H3.3K27M CUT&RUN density shown at the right.

(J) The protein levels of SMARCA4 and SOX10 were not altered to a detectable degree in H3.3K27M-depleted DIPG17 cells. sgNeg: sgRNA targeting *ROSA26* locus; sgH3.3K27M: sgRNA targeting the mutant allele of H*3F3A* gene, but the wild type allele was also deleted based on the literature. α-Tubulin was used as a control.

(K) Depletion of H3.3K27M in DIPG17 cells results in reduced H3K27 acetylation (H3K27ac) and increased H3K27 tri-methylation (H3K27me3). DIPG17 cells in (J) were collected for Western blotting analysis of H3K27ac and H3K27me3.

(L) Few reduced SMARCA4 peaks overlapped with increased H3K27me3 peaks in H3.3K27M-depleted DIPG17 cells. H3K27me3 CUT&RUN was performed in DIPG17 cells with or without deleting H3.3K27M. 10764 H3K27me3 peaks with increased density with a cut off of (sgH3.3K27M)/sgNeg >1.2, FDR <0.05) and 14302 SMARCA4 with reduced density were identified as described in Fig 7G.

(M) Effects of H3.3K27M deletion on H3K27ac levels on chromatin. H3K27ac peaks in H3.3K27M-deleted DIPG17 cells were divided into two groups (reduced and no-difference) based on changes in H3K27ac density compared to sgNeg with a cut off of (sgH3.3K27M)/sgNeg <0.83, FDR <0.05). The H3K27ac CUT&RUN density at each H3K27ac peak of each group was calculated and represented by Heatmap, with average density at all H3K27ac peaks from two independent repeats in each group shown in the right.

(N) The reduced SMARCA4 occupancy was positively correlated with the reduction of H3K27ac levels on chromatin in H3.3K27M-depleted DIPG17 cells. SMARCA4 CUT&RUN peak density ratio FC (sgH3.3K27M)/sgNeg) at shared SMARCA4 and H3K27ac peaks were used for analysis by the Cor. Test function with Pearson method.

(O) Heatmaps showing the SMARCA4 CUT&RUN density at each H3K27ac peak with reduced density or without changes in H3.3K27M-depleted DIPG17 cells identified in (M), with the average density of SMARCA4 CUT&RUN signals from two independent repeats at each group of H3K27ac peaks shown at the right.

(P) Effects of H3.3K27M depletion on Sox10 chromatin binding in DIPG17 cells. The average of two biological replicates were represented.

(Q) Correlations between reduced SMARCA4 occupancy and reduced Sox10 occupancy in H3.3K27M-depleted DIPG17 cells.

Supplementary Table S2. Genes down-regulated in both DIPG6 and DIPG17 after SMARCA4 depletion.

Gene	DIPG17		DIPG6	
	LFC	FDR	LFC	FDR
RP11-12J10.4	-0.58	8.69E-03	-0.61	4.08E-02
FBN2	-0.58	6.80E-15	-0.75	9.88E-07
LDLRAD2	-0.59	6.28E-15	-1.60	3.39E-18
RAB20	-0.59	1.98E-04	-1.45	2.71E-04
NFIC	-0.59	2.01E-10	-0.82	1.87E-03
DNAJC22	-0.59	1.67E-05	-0.72	2.89E-02
DPYSL2	-0.59	4.30E-12	-0.65	1.91E-02
THRA	-0.59	5.14E-15	-0.64	4.80E-04
PPP1R1B	-0.59	2.66E-02	-0.91	4.24E-04
LAMC3	-0.59	1.56E-09	-0.73	2.61E-05
CERS4	-0.60	2.99E-08	-0.60	7.44E-04
GAS7	-0.60	5.05E-11	-0.86	6.52E-04
CELSR2	-0.61	1.06E-09	-0.62	1.92E-02
CHD4	-0.61	1.24E-24	-0.64	1.29E-02
HLA-B	-0.61	5.11E-17	-1.03	4.43E-05
MRAP2	-0.61	1.65E-05	-1.18	4.06E-06
FLNA	-0.62	1.71E-110	-0.58	1.77E-02
RP5-940J5.6	-0.63	4.44E-16	-0.59	4.53E-04
LGALS3BP	-0.63	1.09E-13	-1.13	4.51E-17
ACACB	-0.64	1.87E-05	-1.34	6.61E-05
TNFRSF12A	-0.64	1.55E-14	-0.97	1.30E-08
CA12	-0.64	5.82E-18	-0.93	2.11E-04
NRM	-0.65	1.70E-09	-0.76	3.11E-06
TMEM159	-0.65	8.81E-05	-1.08	1.09E-06
PROCR	-0.65	4.13E-05	-0.75	4.91E-02
LAMA1	-0.65	1.01E-12	-0.92	3.42E-08
LPL	-0.65	2.21E-12	-0.80	1.27E-03
SPINT1	-0.66	1.03E-02	-0.76	3.53E-02
HTR6	-0.66	1.02E-02	-1.15	3.61E-04
CEP295NL	-0.66	1.22E-10	-0.60	2.05E-04
CTD-2515O10.5	-0.67	1.32E-10	-0.72	1.04E-04
GRAMD1A	-0.67	2.46E-19	-0.65	1.44E-02
NLRC5	-0.68	7.20E-05	-0.76	7.03E-03
CCT6P1	-0.68	3.61E-03	-0.67	2.50E-02
TKT	-0.69	1.57E-25	-0.61	2.24E-02
BSG	-0.69	3.79E-47	-0.82	4.35E-05
SRPX	-0.69	5.09E-20	-1.49	5.37E-15
RP11-781P6.1	-0.69	9.83E-03	-0.91	4.02E-02
NELL2	-0.69	5.19E-10	-0.65	1.27E-03
RPS6KA1	-0.69	3.36E-18	-0.71	7.17E-05
HSPG2	-0.69	9.50E-24	-1.69	1.42E-11
SLC44A5	-0.69	6.35E-03	-2.00	6.23E-03
APOBEC3B	-0.70	1.66E-06	-0.83	3.46E-08

CRYAB	-0.70	7.96E-05	-1.26	1.42E-10
GNAO1	-0.70	1.47E-02	-1.09	1.66E-03
LTBP4	-0.71	1.31E-15	-1.37	1.26E-07
LIFR	-0.71	3.09E-23	-0.66	8.37E-05
RP11-42O4.2	-0.71	2.54E-03	-1.11	3.37E-02
NEDD9	-0.71	5.56E-12	-1.74	8.43E-07
SOD3	-0.74	2.20E-11	-3.49	3.48E-03
TIMP2	-0.74	7.74E-15	-0.63	1.93E-02
TUBA4A	-0.74	3.75E-06	-0.98	5.94E-05
ASPHD1	-0.75	9.87E-07	-2.09	7.22E-11
SCARA3	-0.75	1.43E-23	-0.68	4.80E-06
IFITM2	-0.75	1.58E-11	-2.90	2.53E-59
TMEM31	-0.75	2.86E-02	-1.28	3.75E-02
CISH	-0.76	8.04E-04	-0.96	1.08E-02
FXYD5	-0.77	1.38E-06	-1.21	1.02E-16
KCNS3	-0.77	3.91E-05	-1.51	9.56E-07
PHF19	-0.78	9.16E-18	-0.71	1.01E-02
APOBEC3A	-0.78	1.90E-03	-0.92	7.93E-07
SCN1B	-0.79	4.73E-02	-0.91	6.83E-05
ZFPM2	-0.79	5.52E-10	-0.61	7.56E-04
BICD1	-0.79	7.95E-24	-0.58	3.41E-04
KRT8	-0.80	3.64E-09	-0.99	1.94E-02
DRAXIN	-0.80	4.52E-18	-1.69	1.24E-22
PELI3	-0.81	2.87E-07	-1.01	1.04E-04
HTRA1	-0.81	1.12E-26	-1.09	3.99E-07
RAMP2	-0.82	1.20E-04	-0.60	8.37E-03
ALDH16A1	-0.83	2.07E-14	-0.71	1.36E-05
ITPR3	-0.84	3.60E-29	-0.78	1.22E-05
RP11-162P23.2	-0.84	5.57E-09	-0.78	3.04E-06
TFCP2L1	-0.85	6.40E-07	-1.20	8.87E-15
SERPINH1	-0.85	2.34E-53	-1.34	2.63E-05
C12orf75	-0.85	8.18E-14	-0.71	2.91E-04
RP11-402D21.2	-0.85	3.63E-18	-0.99	2.12E-11
AGRN	-0.85	1.42E-28	-0.80	1.44E-03
TAGLN3	-0.85	2.17E-24	-0.86	6.18E-04
MSN	-0.86	2.04E-54	-0.64	1.45E-02
MYLK	-0.86	5.03E-06	-0.83	2.98E-02
SPEG	-0.86	1.66E-21	-0.66	5.47E-03
SEMA3D	-0.86	1.15E-07	-0.65	8.20E-04
COL18A1	-0.87	4.59E-31	-1.09	2.94E-15
CTD-3148I10.9	-0.87	4.47E-05	-0.68	2.28E-03
STAC2	-0.87	5.22E-05	-1.38	1.85E-14
ISLR2	-0.88	2.31E-11	-0.87	6.29E-03
RP11-54O7.14	-0.88	3.45E-25	-0.79	7.46E-07
FGFR2	-0.88	5.82E-24	-0.94	3.24E-07
ALDH2	-0.88	2.69E-20	-0.77	7.63E-08
CTA-150C2.16	-0.88	4.31E-04	-0.75	8.26E-05
CRTAP	-0.88	1.33E-25	-0.79	1.44E-03

MASP1	-0.89	2.36E-07	-1.45	1.68E-02
VASN	-0.89	2.55E-06	-1.38	1.05E-04
WWP2	-0.89	1.88E-35	-1.46	1.14E-04
CDH4	-0.90	6.60E-04	-0.91	4.82E-10
CCNB1IP1	-0.91	5.35E-34	-1.08	3.28E-06
MT-TV	-0.91	9.19E-06	-0.59	3.66E-03
MYH7	-0.92	7.38E-04	-1.42	1.33E-10
FGFBP3	-0.92	3.73E-28	-1.03	9.21E-06
GLB1L2	-0.93	1.16E-21	-0.98	4.97E-11
LINGO3	-0.95	1.53E-02	-0.72	2.74E-03
AEBP1	-0.95	1.26E-32	-0.95	6.53E-05
ADAM15	-0.96	1.39E-28	-1.04	9.56E-07
ME1	-0.96	1.67E-39	-1.31	4.05E-10
POPDC3	-0.97	1.03E-16	-1.05	6.14E-05
NOV	-0.97	5.98E-09	-1.94	1.09E-18
CNTFR	-0.99	7.89E-05	-2.03	2.79E-48
AC009469.1	-0.99	5.16E-04	-1.59	1.11E-07
ARHGEF16	-1.00	1.54E-17	-1.05	1.22E-03
PTPN14	-1.01	1.10E-43	-0.76	4.78E-06
RP11-627J17.1	-1.02	7.52E-15	-0.68	7.55E-03
NID1	-1.02	2.71E-31	-0.96	1.14E-04
FGFR4	-1.02	4.95E-31	-1.49	7.09E-16
MMP2	-1.03	1.52E-46	-0.63	3.89E-04
LHX6	-1.04	4.70E-18	-2.37	1.01E-03
PRDM8	-1.05	7.40E-08	-2.89	2.16E-02
RP11-298A10.3	-1.06	1.08E-06	-1.05	1.82E-02
BST2	-1.06	1.36E-16	-2.19	8.24E-05
MT-TS1	-1.07	2.45E-33	-0.73	1.44E-03
KIAA1161	-1.07	4.67E-52	-1.39	6.36E-06
ZCCHC17	-1.09	5.35E-54	-0.73	7.81E-07
FBLN2	-1.11	4.32E-30	-0.94	7.67E-11
RXRG	-1.11	3.18E-19	-2.10	1.18E-04
TYRO3	-1.12	1.32E-34	-0.71	3.90E-03
RP11-266K22.2	-1.13	3.40E-37	-0.63	1.48E-03
MAGI2	-1.15	1.68E-18	-0.73	3.07E-05
RP11-212I21.3	-1.15	1.61E-16	-0.59	1.57E-02
RP11-25K21.4	-1.16	4.69E-02	-1.55	2.46E-02
NUDT8	-1.16	1.34E-07	-1.21	3.08E-04
KB-1183D5.12	-1.16	3.75E-03	-2.92	3.16E-02
SGK3	-1.17	1.87E-32	-0.73	3.15E-02
INPP5J	-1.18	6.16E-07	-1.75	1.93E-06
RTN4R	-1.19	8.61E-15	-1.68	2.55E-10
PSTPIP2	-1.19	1.75E-22	-0.65	3.29E-03
TNS1	-1.21	4.65E-19	-1.68	3.57E-25
RP11-61L23.2	-1.22	5.20E-11	-0.96	1.22E-02
COL2A1	-1.23	4.28E-68	-0.98	3.49E-10
RAB3A	-1.23	6.15E-20	-1.21	1.92E-04
PTGS1	-1.24	1.05E-05	-1.95	8.77E-17

SHMT1	-1.25	5.80E-46	-0.62	2.51E-03
METRN	-1.26	3.89E-17	-0.67	1.19E-02
MAMLD1	-1.27	1.05E-15	-0.88	1.51E-06
RP11-480I12.5	-1.28	4.62E-07	-0.81	5.95E-03
NGEF	-1.32	1.95E-08	-1.55	2.20E-13
KLHL26	-1.32	1.80E-11	-1.77	8.52E-13
RFX4	-1.34	2.90E-10	-1.88	3.95E-07
AFAP1L1	-1.36	1.93E-49	-1.16	4.66E-08
PCDH20	-1.38	1.93E-09	-1.27	7.38E-08
RP11-310K10.1	-1.38	1.93E-09	-1.28	6.37E-08
RP11-696D21.2	-1.39	3.37E-08	-3.28	1.98E-03
OSBPL10	-1.40	4.55E-33	-0.81	2.61E-05
SCN4B	-1.41	5.24E-07	-0.93	7.67E-03
ITGA7	-1.43	1.69E-58	-1.59	7.53E-20
FXYD3	-1.43	2.09E-04	-1.54	2.10E-05
EPHA8	-1.45	1.06E-02	-0.78	4.30E-02
MRPS18A	-1.45	2.02E-60	-0.89	3.73E-09
RP11-298A10.1	-1.46	9.88E-15	-1.70	5.98E-05
AC099548.6	-1.49	9.10E-17	-1.50	3.03E-05
RASSF2	-1.50	4.13E-46	-0.98	4.87E-05
CCDC136	-1.50	3.43E-09	-0.65	1.16E-02
SFRP2	-1.52	2.22E-72	-1.85	1.70E-22
RSPH9	-1.54	7.88E-77	-0.91	3.79E-09
RP11-482D24.3	-1.54	6.90E-05	-2.51	1.50E-06
ARHGAP24	-1.55	1.07E-16	-1.68	9.76E-03
RHOJ	-1.57	5.39E-101	-1.79	2.42E-16
GBGT1	-1.58	9.09E-11	-1.27	3.44E-12
TCAF2	-1.59	2.49E-33	-1.68	1.03E-05
HHIP	-1.59	2.91E-26	-0.63	1.72E-03
APLN	-1.66	4.64E-20	-1.11	1.13E-02
FREM1	-1.69	8.67E-22	-2.38	1.76E-38
RPE65	-1.76	3.63E-04	-1.89	4.38E-03
MRO	-1.77	1.14E-21	-0.94	6.18E-03
CDHR1	-1.77	4.16E-62	-0.98	4.62E-07
NEURL1	-1.83	6.38E-06	-1.23	1.38E-04
PRUNE2	-1.85	3.97E-21	-1.72	2.22E-09
IL6R	-1.88	2.53E-28	-1.03	1.38E-04
TLR4	-1.91	8.07E-03	-0.93	4.20E-03
PYROXD2	-1.92	2.33E-14	-1.36	1.88E-02
TNN	-1.96	7.98E-09	-1.46	5.54E-04
LGI4	-2.04	1.09E-09	-1.29	1.21E-03
PCA3	-2.07	4.47E-06	-1.74	2.00E-03
CHST9	-2.09	5.00E-20	-1.88	2.35E-25
RP5-877J2.1	-2.13	5.42E-29	-0.94	1.45E-02
C16orf89	-2.14	3.68E-06	-2.49	8.09E-05
TEX19	-2.15	3.38E-12	-2.24	2.14E-02
SMARCA4	-2.15	1.94E-14	-2.08	2.22E-07
GPR78	-2.27	1.85E-02	-1.34	4.18E-03

BANCR	-2.28	8.50E-03	-3.44	4.66E-02
ACKR3	-2.28	3.30E-65	-1.35	4.94E-08
FCGR2A	-2.32	1.67E-55	-1.02	4.61E-02
PLA2G3	-2.39	1.80E-150	-0.80	2.83E-06
AMER2	-2.66	1.78E-07	-0.60	1.37E-03
TNFAIP6	-2.88	2.57E-09	-1.31	5.61E-16
SLC14A1	-3.14	1.08E-17	-1.62	2.10E-07
ATP1A2	-3.55	6.06E-38	-1.74	8.51E-18
GPR174	-3.75	1.44E-07	-1.56	2.23E-04
AZGP1	-4.43	8.35E-91	-2.47	3.91E-19
ENPP6	-5.45	3.12E-02	-1.32	1.59E-06

Supplementary Table S3. Oligonucleotides used in this study. Related to STAR Methods.

Primers	Sequence (5’-3’)	
SFRP2-qRT-PCR forward primer	CTGCCACCGCTTCACCGAGG	
SFRP2-qRT-PCR reverse primer	CCAGCCACCGAGGAAGCTCCA	
HSPG2-qRT-PCR forward primer	TGTGTCGAGATGGAATCAAAGGA	
HSPG2-qRT-PCR reverse primer	GTCGGACTCTGCTATGCCATGT	
COL2A1-qRT-PCR forward primer	CCGAGGCAACGATGGTCAGC	
COL2A1-qRT-PCR reverse primer	TGGGGCCTTGTTCACCTTTGA	
LTBP4-qRT-PCR forward primer	GACGGCTACTCAGATGCCTC	
LTBP4-qRT-PCR reverse primer	GCCTCTGAGATCACGTGTTGG	
ITGA7-qRT-PCR forward primer	GGGCAGCAAGGTCAAGTATG	
ITGA7-qRT-PCR reverse primer	AGGCCACATGATGTTGAGGA	
COL18A1-qRT-PCRforward primer	GTGCCCATCGTCAACCTCAA	
COL18A1-qRT-PCR reverse primer	CCGTCAAAGGAGAAGATGCGT	

β-ACTIN-qRT-PCR forward primer	AGAGCTACGAGCTGCCTGAC	
β-ACTIN-qRT-PCR reverse primer	AGCACTGTGTTGGCGTACAG	
C&R-SFRP2-forward primer	TCCAAGGCCAAGGCGTTTAC	
C&R-SFRP2-reverse primer	CAGCATACACGTTTGTAGGGC	
C&R-HSPG2-forward primer	CCTGACCCCCATCCCAGATA	
C&R-HSPG2-reverse primer	CCTGACTACCGTGGATGCAA	
C&R-COL2A1-forward primer	AACCGGATCCCCTAGGTGTG	
C&R-COL2A1-reverse primer	CTTATACGGCCCTGCGGTAAT	
Negative-forward primer	TGCAAAATTTATTTGGGAGAAAA	
Negative-reverse primer	AGCTGCCATATAGAAAATTGGTC	
sgNeg	GAAGATGGGCGGGAGTCTTC	
sgSMARCA4-1	GAACAAGCTTCCCGAGCTCT	
sgSMARCA4-2	GAAGATTACTTTGCGTATCG	
sgEZH2-1	CAAGATGAAGCTGACAGAAG	
sgEZH2-2	GTGGTGGATGCAACCCGCAA	
sgPCNA	GGACTCGTCCCACGTCTCTT	
sgH3.3K27M	GAGGGCGCACTCATGCGAG	
sgSOX10-1	CAAGCGCCCCTTCATCGAGG	
sgSOX10-5	CCGCTCAGCCTCCTCGATGA	
sgPBRM1-P7	GCAATGGTCTTGAGATCTAT	
sgPBRM1-P12	ATAGATCTCAAGACCATTGC	
sgSMARCA2-1	AGTGGTGATTCTTCATTCGG	

sgSMARCA2-2	AAGACCGAGCTCACCGCATC	
sgBRD9-B5	TTCATGGTGCCAAAATCCAT	
sgBRD9-B6	GCGAAGAAGATCCTTCACGC	
sgARID1A-1	CAGACACATAGAGGCGATAG	
sgARID1A-2	ACCACCCAGCTCATACAACT	
sgSS18-2	TACGGGGACCAATACAGTCA	
sgSS18-3	CAGAATATGCCTATGGGTCC	
sgSMARCE1-1	CTTTCTGCTGTACCTCATGT	
sgSMARCE1-2	GAGATTGGCAAGATTATTGG	
sgmSMARCA4	CGCGCTCATCACATACCTCA	
sgSFRP2-1	TAGGTCATCGAGGCAGACGG	
sgSFRP2-1	TGAGTGCGACCGTTTCCCCC	
shLTBP4-1	CAACCGGCTTTGAAAGAGTTA	
shLTBP4-2	CCCAGACTTAGGTCCACCTTA	